Article

pubs.acs.org/Biomac

Early Stiffening and Softening of Collagen: Interplay of Deformation Mechanisms in Biopolymer Networks

Nicholas A. Kurniawan,*[,†,‡] Long Hui Wong,[‡] and Raj Rajagopalan[†,‡,§]

[†]NUS Graduate School for Integrative Sciences and Engineering, Singapore 117456

[‡]Singapore-MIT Alliance and [§]Department of Chemical and Biomolecular Engineering, National University of Singapore, Singapore 117576

Supporting Information

ABSTRACT: Collagen networks, the main structural/mechanical elements in biological tissues, increasingly serve as biomimetic scaffolds for cell behavioral studies, assays, and tissue engineering, and yet their full spectrum of nonlinear behavior remains unclear. Here, with self-assembled type-I collagen as model, we use metrics beyond those in standard single-harmonic analysis of rheological measurements to reveal strain-softening and strain-stiffening of collagen networks both in instantaneous responses and at steady state. The results show how different deformation mechanisms, such as deformation-induced increase in the elastically active fibrils, nonlinear extension of individual fibrils, and slips in the physical cross-links in the network, can lead to the observed complex nonlinearity. We demonstrate how comprehensive rheological analyses can uncover the rich mechanical properties of biopolymer networks, including the above-mentioned softening as well as an early strain-stiffening, which are important for understanding physiological response of biological materials to mechanical loading.

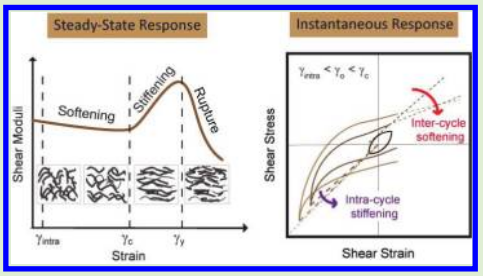

INTRODUCTION

Cells are known to sense, respond to, and even actively modulate the physical and mechanical microenvironment of the surrounding matrices.[1,2] These mechanosensory and mechanotransduction actions underlie various physiological processes, including regulation of the internal stiffness of the cell and cell motility, morphology, proliferation, and differentiation.[3−5] Breakdown of these functions can lead to diseases, with cancer as a most notable example. A thorough understanding of the relation of both intra- and extra-cellular materials to cell functions is therefore essential not only for cell behavioral studies but also for rational designing of biocompatible scaffolds in tissue engineering. Correspondingly, the importance of understanding the mechanical properties of these biomaterials has been increasingly appreciated.[6] To this end, fiber networks of biologically relevant proteins have proven to be excellent model systems that provide valuable insights, for example, into the origin of cytoskeletal mechanics.[7,8] Recent experimental studies on biopolymer fiber networks reconstituted in vitro have highlighted that, like many biological materials, these networks stiffen when strained, thereby maintaining their mechanical integrity.[9]

Collagen is the most abundant extracellular protein and has been commonly used as biomimetic scaffolds for in vitro cell cultures, assays, and tissue regeneration.[10,11] It has been shown that collagen fiber networks exhibit strain-stiffening behavior similar to that of other biopolymer networks,[12−14] a behavior that bodes well for collagen's well-known function as a key structural and mechanical support in the body. Collagenous tissues, such as tendons, ligaments, skin, and various connective tissues, have long been documented to be crucial load-bearing components, under both steady-state and dynamically varying loadings, as a result of large-scale bodily movements as well as small-scale cell activities, with nonlinear stress−strain relations.[15,16] Despite the obvious importance of thorough characterization of the nonlinear mechanics of collagen networks, the underlying biophysical mechanisms for the strain-dependent behaviors and strain transmission are not well understood.

In this work, we investigate the nonlinear rheological response of self-assembled collagen networks under oscillatory shear over a broad range of strain amplitude and report previously overlooked softening and stiffening phenomena. As a model of collagen fibrillar networks, we use type I collagen, the most abundant type of collagen in noncartilaginous tissues. Rheology was chosen over other mechanical testing options not only because of its widespread use in the mechanical characterization of soft biomaterials but also for the possibility of dynamic viscoelastic measurements of the rather fragile collagen networks self-assembled in situ. We examine the peculiar strain-dependent behavior of the networks, which includes both strain-softening and strain-stiffening, as a function of the applied cyclic strain amplitude. Moreover, by analyzing the raw stress−strain waveforms within each loading cycles directly, we find evidence of early network stiffening that is often masked by overall intercycle softening. We systematically

Received: November 10, 2011
Revised: January 9, 2012
Published: January 31, 2012

quantify this effect with the help of additional measures of elasticity, which should help in the interpretation of the rheological data for other biopolymer systems and soft tissues.

MATERIALS AND METHODS

Preparation of Collagen Gels. Sterile rat tail collagen type I was obtained from BD Biosciences (Bedford, MA) at a concentration of 9.03 mg/mL in 0.02 N acetic acid. Appropriate amounts of the collagen stock solution were mixed on ice with 10× phosphate-buffered saline (PBS), 1 N NaOH, and 1× Dulbecco's modified Eagle's medium (DMEM) to reach a final collagen concentration of 3.5 mg/mL at pH 7.4. All solutions were prepared and kept on ice prior to collagen gelation and rheological tests. For cross-linked collagen networks, appropriate amount of 25% (v/v) glutaraldehyde was added to the collagen mixture in place of DMEM to obtain a final cross-linker concentration of 1% (v/v). The observed microstructural features of the formed collagen networks were similar to those reported in the literature (Figure S1 in the Supporting Information).

Rheological Experiments. Rheological measurements were done using a stress-controlled AR-G2 rheometer (TA Instruments, New Castle, DE) fitted with 40 mm parallel-plate geometry and 500 μm gap size. We polymerized collagen networks in situ by loading 630 μL of the prepared collagen solutions onto the precooled Peltier stage and raising the temperature to 37 °C. Care was taken to avoid the formation of air bubbles, and a solvent trap was used to minimize the effect of dehydration. All measurements were subsequently conducted at 37 °C after allowing 90 min for gelation. Preliminary time-sweep measurements at a frequency of 1 rad/s and small strain amplitude of 1% were done to monitor the time scale of network self-assembly and to ensure that plateau modulus was reached within 90 min, consistent with a previous study.[17] Oscillatory frequency sweeps were performed in the frequency range of 10^{-1} to 10^{2} rad/s at 1% strain amplitude. Strain-sweeps were carried out by varying the logarithmically spaced strain amplitudes at different scanning frequencies. Geometry inertia can cause significant errors in the calculation of sample torque (and, as a result, stress), especially at high frequencies or low sample viscosities. To avoid any detrimental influence of instrument geometry inertia, we analyzed only the data for which the raw phase angle equals the sample phase angle.[18] This procedure may result in data truncations, especially at high measurement frequencies and large strain amplitudes.

Data Treatment. In rheological measurements, an oscillatory strain

$$\gamma(t) = \gamma_0 \sin(\omega t) \tag{1}$$

with variable amplitude γ_0 is applied to the sample, and one then monitors the resulting stress. In many typical setups, the stress waveform is taken to be sinusoidal $\tau(t) = \tau_0 \sin(\omega t + \delta)$ with a stress amplitude τ_0 and a phase shift δ, as expected for small γ_0. On the basis of the in-phase and out-of-phase components of the response, the viscoelastic properties of the material can then be characterized by the elastic modulus

$$G' = (\tau_0/\gamma_0) \cos \delta \tag{2}$$

and the loss modulus

$$G'' = (\tau_0/\gamma_0) \sin \delta \tag{3}$$

which are measures of the stored and dissipated energy in the network, respectively. At large γ_0, however, the stress−strain response may become nonsinusoidal because of the nonlinearity in the material, as we shall show in the case for collagen networks. In this case, G' and G'' are not uniquely defined, and there are other viscoelastic measures that can assist data interpretation. We employ both the conventional (G' and G'') as well as these additional measures, which are introduced later, to understand the nonlinear behavior of collagen networks.

RESULTS

The overall rheological response of a collagen network is illustrated and highlighted using a network of a fixed collagen concentration (3.5 mg/mL) in Figure 1. Strain-sweep measurements were performed over more than two orders of magnitude

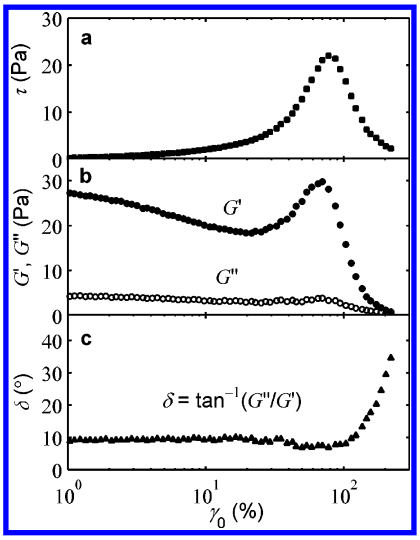

Figure 1. Rheological response of collagen network under oscillatory shear with varying strain amplitude γ_0. (a) The stress τ, (b) the storage G' (filled circles) and loss G'' (open circles) moduli, and (c) the phase angle δ are plotted against γ_0. The network was polymerized at 3.5 mg/mL concentration and pH 7.4. The measurement was made at 37 °C and ω of 1 rad/s, with logarithmically increasing γ_0. For clarity, only every third data point is shown.

of strain amplitude γ_0. For all $\gamma_0 \lesssim 250\%$, the elastic or storage modulus G' is much larger than the viscous or loss modulus G'', showing the predominantly elastic nature of the network. The ratio between G'' and G', represented in terms of the phase angle δ and shown in Figure 1c, illustrates the clear nonlinear behavior of both G' and G'' with respect to γ_0. In particular, at small strain amplitudes, G' decreases from 27 Pa at $\gamma_0 \approx 1\%$ to 18 Pa at $\gamma_0 \approx 20\%$, indicating strain-softening of the network, and this softening is followed by strain-stiffening, indicated by the upturn of G' to 30 Pa at $\gamma_0 \approx 75\%$. This strain-dependent trend is also found in G'' (i.e., shear-thinning and shear-thickening), although the corresponding extents of softening and stiffening are not equal to those in G'. The critical strain γ_c signifying the onset of stiffening in both G' and G'' is found to be ∼20%, consistent with a recent report.[19] Beyond $\gamma_0 \approx 75\%$, there is a sharp decrease in τ, G', and G'', implying network rupture, which will not be further discussed in this Article. We denote this level of strain, beyond which the network yields, by γ_y.

The strain-stiffening behavior is characteristic of many biopolymer networks,[9] although the mechanisms responsible for this phenomenon are still debated. However, the softening of biopolymer networks at small strains is unexpected, and we find that such softening is reported only rarely, and in passing, in the literature.[8,20] In the case of collagen, the experiments of Barocas et al. do indicate slight softening in the strain-sweep result, although the authors make no mention of it.[21] In general, the softening of collagen networks has never been reported in the literature, to our knowledge. We suspect that the common practice of plotting sparse data points of G' and G'' on logarithmic scale, as well as the use of different concentration ranges, collagen sources, and cross-linking states of collagen, might have obscured the softening effects or might have contributed to their being undetected. In what follows, we

denote the G' and G'' values at the lowest tested γ_0, namely, 1%, as G'_0 and G''_0, respectively, to assist in further analyses. Both G'_0 and G''_0 values are comparable to prior reports on rat tail collagen type I.[13,22]

To examine the influence of the measurement time scales, we also carried out measurements at different frequencies ω. The storage and loss moduli, normalized against G'_0 and G''_0 and shown in Figure 2, show clearly that the overall trend of strain-

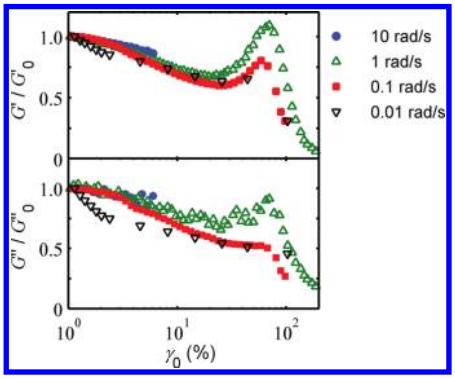

Figure 2. Strain dependence of G' and G'' at different scanning frequencies. The data are normalized against G'_0 and G''_0 to account for sample-to-sample variations in G' and G''. The data for ω = 10 rad/s are truncated at γ_0 = 6%, beyond which instrument inertial effects start to affect the experimental results.

softening, strain-stiffening, and rupture is preserved, although the degree of the softening and stiffening varies. In addition, the two characteristic strains that describe the nonlinear features, namely, γ_c and γ_y, do not seem to be a function of ω, at least for $\omega \leq 1$ rad/s. These observations suggest that for the time scales probed in this study the microstructural deformation mechanisms responsible for the strain-dependent and stress-relaxation behaviors of the networks are self-consistent and are little affected by the frequency of measurement. Indeed, the small-strain G'_0 and G''_0 of collagen networks exhibit weak frequency dependence, as shown in Figure S2 in the Supporting Information and reported elsewhere.[17,23] In addition to the small magnitude of the measured value of the phase angle δ (~9°) at small γ_0 (Figure 1c), the above-mentioned behavior is characteristic of physical networks with transient cross-links in the form of noncovalent interactions.[24] Whereas analyses of the nonlinear behavior of the networks at different frequencies may shed light on interesting time-dependent properties of these interchain interactions, detailed quantitative measurements are currently limited by instrument inertia at high frequencies and prohibitively long measurements required at low frequencies. For the remainder of this Article, we shall therefore focus on measurements at ω = 1 rad/s.

We now proceed to investigate the reversibility of the nonlinear behaviors to examine whether or to what extent the material has a structural memory of the loading history. Figure 3 shows the rheological response of the networks under three different cyclic protocols. First, γ_0 was logarithmically increased from 1 to 15% and then decreased back to 1% (Figure 3, Panel 1). Because $\gamma_c \approx 20\%$, only strain-softening is expected and is observed. The reversibility in this strain regime is almost complete, and the final G' and G'' are only slightly lower than the initial values by ~10% for both moduli (Figure 3a,d). As a result, there is a negligible change in δ (Figure 3g). In the second protocol, γ_0 was logarithmically increased from 1 to 60%

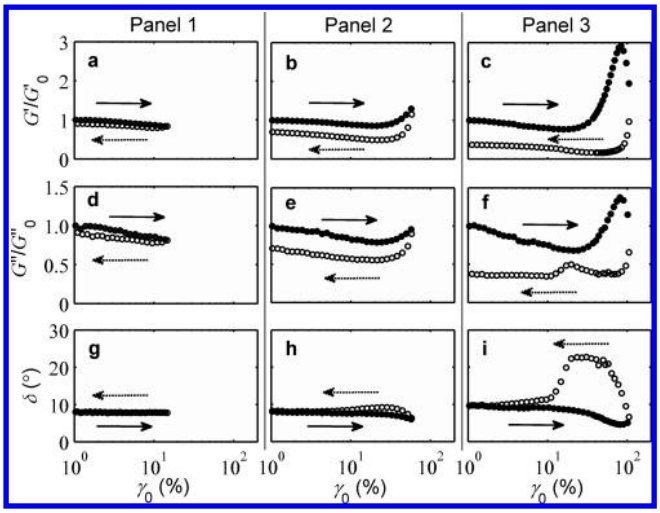

Figure 3. Reversibility of the network under oscillatory shear rheology. Normalized shear moduli, G' (a–c) and G'' (d–f), and the phase angle δ (g–i) are plotted against strain amplitude γ_0. Strain was initially increased logarithmically (filled circles) to a maximum γ_0, as indicated by the solid arrows, and was then decreased back (open circles) to the minimum γ_0 of 1%, as indicated by the dashed arrows. The maximum γ_0 is specified at 15 (Panel 1), 60 (Panel 2), and 105% (Panel 3). All measurements were done at ω of 1 rad/s.

before decreased back to 1% (Figure 3, Panel 2). The maximum γ_0 now is larger than γ_c but smaller than $\gamma_y \approx 75\%$. Partial strain-stiffening is observed in both G' and G'', as expected (Figure 3b,e). One observes a reduced reversibility in this case, with the final G' and G'' being about 70% of the initial values. Interestingly, the initial and final δ values at γ_0 = 1% are almost identical (Figure 3h), suggesting that the initial and final networks are structurally similar, despite having undergone strain-stiffening. In the third protocol, γ_0 was increased from 1 to 105% and decreased back to 1% (Figure 3, Panel 3). The maximum γ_0 is now larger than γ_y, and network yield is observed, as expected. As a result, the irreversibility in G' and G'' is even more severe, the final values being roughly 64% lower than the initial values (Figure 3c,f). The initial and final δ values, however, are again very close to each other (Figure 3i). Taken together, our findings suggest that the varying degree of reversibility with maximum γ_0 is related to the prior network deformation mechanisms (loading history) that have taken place. Similar behavior has been observed in elastomers and has been linked with the pseudoelasticity theory that takes into account material anisotropy induced by periodic loading.[25] We shall discuss the structural basis for the above observed behavior of collagen in more detail below.

Plots of instantaneous stresses $\tau(t)$ against strains $\gamma(t)$, often called Lissajous–Bowditch plots, for different γ_0 values allows one to follow the actual network response each loading cycle during the oscillatory shear testing. For purely elastic materials, the response is expected to be completely in phase (δ = 0) and, as a result, the Lissajous–Bowditch plot collapses to a line with a slope of G'. The response of purely viscous materials is expected to be out of phase by $\delta = \pi/2$, and the Lissajous–Bowditch plot becomes a circle. Viscoelastic materials like biopolymer networks exhibit both elastic and viscous properties, and the Lissajous–Bowditch plot is expected to be a perfect ellipse, with the magnitude of the complex modulus $|G^*|$ as the slope of the semimajor axis.[26] Observation of the shape of the Lissajous–Bowditch plots is therefore a

dx.doi.org/10.1021/bm2015812 | Biomacromolecules 2012, 13, 691–698

convenient tool to monitor the evolution of the dynamic viscoelasticity of the examined material. It is important to note, however, that the above behaviors hold only as long as the stress−strain waveform is strictly a single-harmonic sinusoidal, as is the case when the mechanical behavior is linear. In collagen networks, as shown in Figure 4, such elliptical

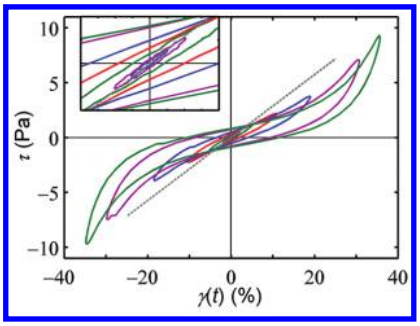

Figure 4. Lissajous−Bowditch plots generated from the stress−strain waveforms at different γ_0. The inset is a zoom in for $|\gamma| < 4\%$, showing the ellipses as expected in the linear viscoelastic regime. For $\gamma_0 > 5\%$, the Lissajous−Bowditch plot becomes increasingly distorted, indicating nonlinear behavior. The dotted line is extrapolated from the semimajor axis of the innermost ellipse.

Lissajous−Bowditch plots are only observed at small γ_0; oscillations with larger strain amplitudes γ_0 lead to increasingly distorted response. Deviation from ellipticity is characteristic of nonlinear viscoelastic response.[26] In this Article, we denote the instantaneous response within each cycle at fixed γ_0 as intracycle response and the network response at different γ_0 values as intercycle response.

To illustrate more clearly the deviation of the Lissajous−Bowditch plots from ellipticity, we show in Figure 5 representative Lissajous−Bowditch plots at different γ_0 values, along with the corresponding fitted ellipses obtained based on the assumption that the responses are single-harmonic. The results show that below $\gamma_0 < 5\%$ (e.g., Figures 5a,b) the data can be described well by ellipses, indicating sinusoidal response. Between $5\% < \gamma_0 < 20\%$ (e.g., Figure 5c), where one previously observed (intercycle) strain-softening (Figure 1), the Lissajous−Bowditch plot deviates from the ellipse. This effect becomes more pronounced as γ_0 increases (e.g., Figures 5d−f). Specifically, the slope of τ with respect to γ becomes larger at larger strains, resulting in upwardly convex curves for positive strains, indicative of network stiffening. Interestingly, such intracycle network stiffening behavior begins to appear well under γ_c, below which one might expect only strain-softening behavior (Figure 1). This apparent contradiction is a result of the assumption mentioned previously that the resulting stress−strain waveform is strictly sinusoidal.

Various methods are available to probe the nonsinusoidal stress−strain waveform at large oscillation amplitudes. One experimental option is to apply a steady prestress to the material, rather than applying a large-amplitude oscillation, and to measure the mechanical properties by monitoring the linear response upon the application of small, additional oscillation.[27] The measured modulus is called differential modulus, which is conceptually similar to taking the local derivative of the stress. However, this method does not account for the viscous relaxation and flow of the material upon application of prestress. Alternatively, the nonsinusoidal waveform can be analyzed in terms of Fourier transforms and decomposed into

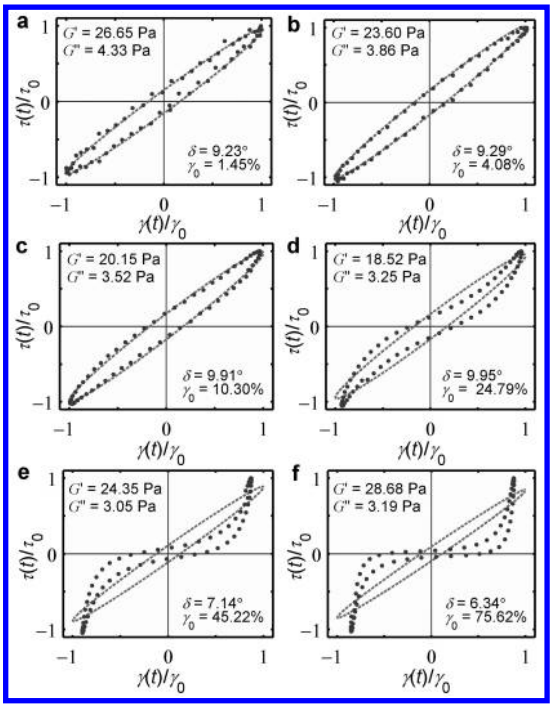

Figure 5. Snapshots of the Lissajous−Bowditch plots under oscillatory shear obtained at different strain amplitudes γ_0. The instantaneous stress $\tau(t)$ and strain $\gamma(t)$ are normalized against the corresponding γ_0 (values are shown) for easy comparison. The raw data (filled circles) are compared with the elliptical fits (dashed lines) based on single-harmonic sinusoids for the stress−strain response. The values of G', G'', and δ obtained on the basis of single harmonicity are also shown for reference. The strain-sweep was done with frequency $\omega = 1$ rad/s.

different harmonic contributions.[28] The sinusoidal approximation used in typical rheological analyses can thus be viewed as taking only the first harmonic response, whereas the nonlinear distortions due to network stiffening arise from the higher harmonic contributions. The drawback of the above decomposition is that the higher harmonic coefficients do not necessarily admit clear physical interpretation of the mechanics.

To address these issues, additional parameters that allow more direct interpretation of the nonlinear phenomena have been introduced.[26] Among these parameters, two moduli are particularly relevant for quantifying the elasticity of the material: the minimum-strain modulus $G'_M = (d\tau/d\gamma)|_{\gamma=0}$ and the large-strain modulus $G'_L = (\tau/\gamma)|_{\gamma=\pm\gamma_0}$. Specifically, G'_M is the tangent modulus at $\gamma = 0$, where the strain rate $\dot{\gamma}$ (and the viscous contribution to τ) is at a local maximum, $d\dot{\gamma}/dt = 0$, and changes in τ are therefore related only to elasticity, whereas G'_L is the secant modulus at the maximum strain $|\gamma| = \gamma_0$, where $\dot{\gamma} = 0$ and the residual stress in the sample results only from the elasticity of the material. These definitions can be easily visualized and compared with the standard first harmonic elastic modulus G'_1 using the Lissajous−Bowditch plot, as shown in Figure 6, and can be conveniently related to the higher harmonic coefficients.[26] At small strains, the Lissajous−Bowditch plot is elliptical, so both G'_M and G'_L converge to the linear elastic modulus, $G'_M = G'_L = G'_1 = G'$. At larger strains, a difference between G'_M and G'_L signifies a nonlinear elastic response. The deviation from the linear viscoelastic response can thus be quantified using an index of nonlinearity, $S \equiv (G'_L - G'_M)/G'_L$, where $S = 0$ indicates linear elastic response, whereas $S > 0$ and $S < 0$ correspond to intracycle strain-

dx.doi.org/10.1021/bm2015812 | Biomacromolecules 2012, 13, 691−698

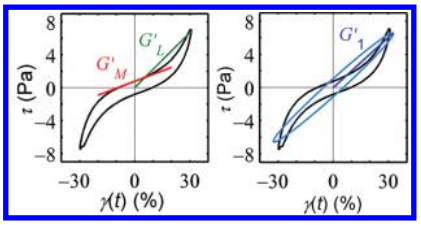

Figure 6. Graphical description of the nonlinear elasticity measures. The left panel shows how G'_M and G'_L are obtained, whereas the right panel illustrates the standard first-harmonic approximation (an elliptical response with a slope of G'_1 along the semimajor axis) and contrasts it with the actual response (black line).

stiffening and softening phenomena, respectively. The upper limit of S is unity and is achieved as $G'_L \gg G'_M$.

We plot the variations of our elastic moduli G'_M, G'_L, and G'_1 for the networks as functions of γ_0 in Figure 7. All three moduli

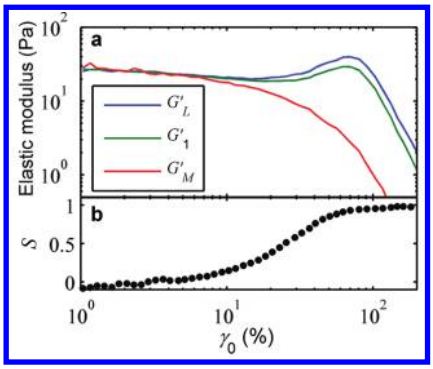

Figure 7. Elastic measures of collagen network as a function of strain amplitude γ_0. In (a), the three elastic moduli G'_1, G'_M, and G'_L are compared. G'_1 falls between G'_M and G'_L, suggesting that it is an average elasticity measure. In (b), the intracycle nonlinearity index S is plotted against γ_0. S increases with γ_0 (intracycle strain-stiffening), even when the elastic moduli decreases with γ_0 (intercycle network softening). There is relatively higher uncertainty (data ripple) in obtaining G'_M and S at small γ_0 due to the numerical calculation of the derivative $d\tau/d\gamma$ at $\gamma(t) \to 0$.

converge as expected in the linear regime and decrease with γ_0 initially, indicating intercycle strain-softening as previously observed. The first-harmonic elastic modulus G'_1 falls between the two other measures throughout, suggesting that it acts as a first-order, average measure of elasticity. Whereas G'_M continues to decrease at large γ_0, G'_1 and G'_L have similar trend of γ_0 dependence and start to increase around $\gamma_0 \approx 15$ and 25%, respectively, indicating strain-stiffening before network rupture. The divergence of G'_M from G'_1 and G'_L marks the onset of nonlinearity around $\gamma_0 \sim 5\%$, much earlier than the strains at which stiffening in both G'_1 and G'_L start to occur. This is confirmed when one plots S as a function of γ_0 in Figure 7b, which shows that S is initially close to zero but that it gradually increases with γ_0, implying the increasing degree of intracycle strain-stiffening of the network. To distinguish it from γ_c, we shall call this strain level that marks the onset of intracycle strain-stiffening as γ_{intra}. It is interesting to note that S never takes on negative values, within experimental error, meaning that no intracycle network softening is observed, although G'_1 reports initial (intercycle) softening before stiffening.

DISCUSSION

In this study, we employ rheology as a tool for investigating the strain-dependent mechanical behavior and the underlying deformation mechanisms in collagen networks. Viscoelastic properties are typically reported in terms of the storage G' and loss G'' moduli. From these two moduli, peculiar behaviors of collagen networks, including strain-softening at small strains, followed by strain-stiffening at larger strains, can be observed. One key rheological property that sheds light on the deformation mechanism is the phase angle δ, which is related to G' and G'' through $\tan \delta = G''/G'$ (see eqs 2 and 3). The phase angle δ is a measure of how much energy is dissipated relative to stored energy. A change in δ as a function of γ_0 therefore reflects the structural changes that lead to strain-induced stiffening or softening in both elastic and viscous responses. Specifically, a decrease in δ implies that there is more energy stored relative to that dissipated, and the decrease has been linked to an increase in the number of elastically active chains.[29] In contrast, an increase in δ suggests that the proportion of dissipated energy increases, which physically could be due to partial breaks in the network. Such relative analysis of the strain-dependent behavior of G' and G'' has been used to investigate the origin of strain-hardening in polymer and filamentous networks.[30,31]

The evolution of δ as a function of γ_0 during the strain-sweep measurements of collagen networks is shown in Figure 1c. Initially δ remains constant at roughly 9° during strain-softening ($\gamma_0 < \gamma_c \approx 20\%$), but decreases significantly from 9 to ~6° at $\gamma_y \approx 75\%$. Beyond γ_y, δ increases sharply. Such a sharp increase in δ is consistent with our previous supposition of network rupture and reflects the increasingly liquid-like behavior of the network, reminiscent of fluidization phenomenon.[32] The observation that δ remains constant for $\gamma_0 < \gamma_c$ suggests that the state of network topology that manifests in the measured viscoelastic properties is not significantly altered in this strain regime. Measurements from our cyclic loading protocol (Figures 3, Panel 1) show that there is a slight irreversibility in G' and G'' but that δ is again unchanged. On the basis of these results, we hypothesize that the observed strain-softening behavior could result from a redistribution of internal stresses through progressive slip of the physical cross-links in the network.[33] If this hypothesis is true, then one would expect that an addition of permanent chemical cross-linkers in the network would diminish the strain-softening effects by reducing the degree of freedom of the entanglement points. This is indeed the case for collagen, as shown in Figure S3 in the Supporting Information. In addition, increasing the frequency of applied strain would restrict the amount of time allowed for such structural relaxation, which explains the decreasing extent of strain-softening with frequency, as we have also observed in Figure 2.

In contrast with the rheological response at small strains ($\gamma_0 < \gamma_c$), δ decreases with γ_0 in the strain-stiffening regime ($\gamma_c < \gamma_0 < \gamma_y$). In addition, the network exhibits partial irreversibility when deformed up to this range of strain, as shown in Figure 3 (Panel 2), the effect of which is more pronounced after network yielding beyond γ_y (Figure 3, Panel 3). These findings suggest the occurrence of a microstructural change, which has been proposed to involve deformation-induced increase in the number of elastically active chains.[29] The increase can be achieved through either recruitment of new collagen fibrils via network remodeling during deformation or engagement of

dx.doi.org/10.1021/bm2015812 | Biomacromolecules 2012, 13, 691−698

previously elastically inactive fibrils when a certain amount of local strain is reached. Numerical simulations on random networks of semiflexible polymer chains have predicted the importance of network arrangement in the overall network elasticity and the associated degree of (non)affinity in the deformation.[34,35] With the recent computational advancements in network imaging in vitro and fibril detection,[12,36] as well as 3-D strain field measurements,[36] a quantitative study on how macroscopic forces are transmitted down to fibril-level deformations would provide an excellent avenue for further analysis of network remodeling during strain-stiffening.

We now turn to the intracycle behavior of collagen networks. Our analysis of the Lissajous–Bowditch plots as a function of increasing γ_0 reveals the existence of another characteristic strain, γ_{intra}, beyond which a departure from single-harmonic stress–strain response in the form of intracycle strain-stiffening ($S > 0$) is observed. Interestingly, for the collagen networks tested in this study, γ_{intra} is smaller than γ_c, implying that for $\gamma_{intra} < \gamma_0 < \gamma_c$ intercycle strain-softening coincides with intracycle strain-stiffening, a seemingly paradoxical result. However, it is important to note that strain-sweep rheological measurements measure the sample's viscoelastic response to steady-state oscillatory shear at varying strain amplitude γ_0, whereas the Lissajous–Bowditch plots reflect the sample's instantaneous response to the oscillatory shear at varying time-resolved $\gamma(t)$. The strain-softening effect in G' (or, equivalently, G'_1), is reproduced even in G'_M and G'_L at small strains as the slope $d\tau/d\gamma$ decreases with γ_0, possibly due to the increase in $\dot{\gamma}|_{\gamma(t)=0} = \gamma_0\omega$.[37] Because collagen networks are predominantly elastic (Figure 1), we do not report the corresponding viscous measures here, for which the strain-rate contribution would need to be carefully considered.[38]

We have already noted (Figure 7) the intracycle strain-stiffening in collagen networks, signified by the nonzero S, for strain amplitudes as small as $\gamma_{intra} \approx 5\%$, well below γ_c. The early strain-stiffening was previously reported by Vader et al.[39] on collagen networks formed from a different source and at a different concentration, but the authors did not attempt a full multiharmonic analysis of their data and left the origin of early strain-stiffening unexplored. Nonellipticity in the Lissajous–Bowditch plots has been reported to be a signature of nonlinear stretching of individual chains in polymer networks.[26] However, it is also possible that the nature and properties of the physical cross-links in the network may contribute to the time-resolved stress–strain waveforms, which may in turn manifest in the intercycle strain-softening behavior and nonelliptic Lissajous–Bowditch plots of the network.

To examine the possible role of the physical cross-links in the instantaneous stress–strain response of the collagen networks, we modify the approach of Schoenberg,[40] who showed that the force response of dynamically cross-linked polymer chains upon a constant-velocity step deformation d is given by

$$\Delta F = n_b\kappa\, d e^{-kt} \quad (4)$$

where $n_b\kappa$ is the stiffness of a permanently cross-linked network and k is the effective rate of cross-link dissociation. In oscillatory rheology, d is sinusoidal and is proportional to shear strain γ given in eq 1. Assuming that superposition is valid, eq 4 can be analytically solved to give the instantaneous force (and therefore stress) response as a function of $\gamma(t)$ for constant k.[41] For weakly cross-linked networks, however, it is likely that the probability of a cross-link dissociation increases with the rate of deformation. Because the functional form is unknown, here we consider a simple model where the dissociation rate k varies linearly with strain rate $\dot{\gamma}$; that is, $k = k_0\, d\gamma/dt$. For sinusoidally varying deformation, one can readily test the validity of this model by examining how G'_M varies with γ_0, since the stress–strain response at $\gamma(t) \to 0$ is mostly contributed by $\dot{\gamma}$. Figure 8 shows that this simple model

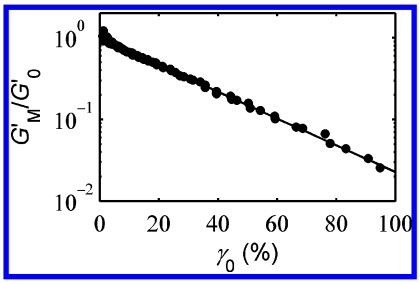

Figure 8. Exponential decay of G'_M with strain amplitude γ_0 for the collagen network. The solid line shows the best fit of the dynamic cross-link model (see text) to the data (filled circles), with a dissociation rate constant k_0 of 60.

can describe the exponential decay of G'_M for an extended range of γ_0 very well, with a best fit, dimensionless dissociation rate constant k_0 of 60. In contrast, when a permanently cross-linked network ($k_0 \to 0$) is assumed, no decay is observed (data not shown), which is consistent with our experimental results for cross-linked collagen network (Figure S3 of the Supporting Information). This result further corroborates the involvement of cross-link dynamics in determining the mechanics of collagen networks. Indeed, we note that degradation and instantaneous reassembly of bonds in transient networks have been successfully used to explain the softening effect during cyclic loading of silk fibers.[42]

We then proceed to check whether the model can account for the nonellipticity of the Lissajous–Bowditch plots. Figure 9

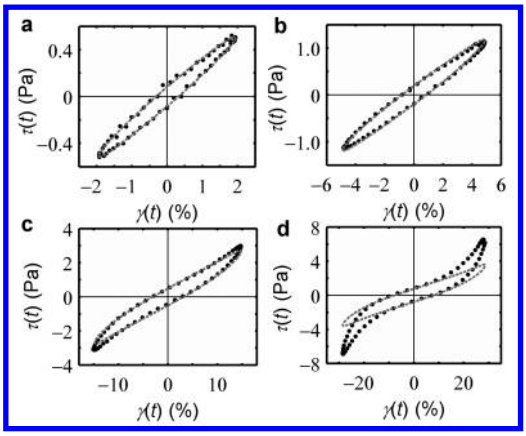

Figure 9. Comparison of the raw Lissajous–Bowditch plots and the cross-link dynamics model of collagen network under oscillatory shear at different strain amplitudes γ_0 values. The raw data (filled circles) are compared with the model (dashed lines) with a dissociation rate constant k_0 of 60. (See text for detail.)

shows a few examples of the comparison between the raw stress–strain data and the model prediction, assuming a dissociation rate constant k_0 of 60. It can be observed that while the model can predict the clockwise overall rotation of the Lissajous–Bowditch plots with γ_0 and can show nonelliptic

dx.doi.org/10.1021/bm2015812 | Biomacromolecules 2012, 13, 691–698

behavior (e.g., Figure 9a−c), it still cannot account for the large degree of nonellipticity at large strains (e.g., Figure 9d). This result suggests that cross-link dynamics play an important role in the observed intercycle softening but that it is not sufficient to fully explain the intracycle stiffening of collagen networks. The stiffening of individual chains, which we have not taken into consideration, has been previously proposed to be responsible for the strain-stiffening of biopolymer networks.[9,43] Considering that individual type I collagen fibrils exhibit nonlinear stiffening properties even at small tensile strains,[44] it seems reasonable to ascribe the large degree of intracycle strain-stiffening behavior of collagen networks to the nonlinear force−extension relation of the individual fibrils. In fact, this is consistent with the observation that below γ_c δ remains unaffected by γ_0, indicating that the microstructural features and connectivity of the network are still largely unperturbed. While a general, constitutive function of the nonlinear force−extension relation in biopolymer chains has not been agreed on, one can, in principle, test this supposition by assuming simple models, such as those proposed in recent studies on various viscoelastic materials,[45−47] and incorporating them in the above deformation scheme. Correspondingly, the observed strain-stiffening, both intra- and intercycle, at $\gamma_0 > \gamma_c$, involves both network rearrangement and stretching of individual fibrils.

CONCLUSIONS

In summary, we have reported previously overlooked strain-dependent viscoelastic behavior of collagen networks under oscillatory shear deformation. Through the use of rheological parameters such as the phase angle, the viscoelastic moduli, and the nonlinearity index, we deduce the different deformation mechanisms that lead to the observed nonlinear mechanical behavior of collagen networks, including strain-softening and strain-stiffening. In particular, the results suggest that the steady-state strain-stiffening behavior of collagen network involves deformation-induced increase in the number of elastically active fibrils via network rearrangement, whereas the early strain-stiffening at small instantaneous strains may well be brought about by the nonlinear stretching of the individual fibrils. Moreover, the strain-softening of collagen at small strains is proposed to arise from the nature of the physical cross-links in the networks. We have identified three characteristic strains that describe these nonlinear features: γ_{intra}, γ_c, and γ_y. Importantly, the frameworks used here provide a more complete and richer picture of the viscoelasticity of collagen networks that is inaccessible from the first-harmonic moduli alone. Such analysis will augment the interpretation of rheological measurements on other (bio)materials, including biopolymer networks of cytoskeletal protein constituents and extracellular matrices. Proper understanding of the strain-dependent mechanical properties of these networks will be beneficial in various cell studies and biomaterial applications.

ASSOCIATED CONTENT

Supporting Information

Microstructure of the self-assembled collagen network as imaged using confocal reflectance microscopy; frequency dependence of the storage and loss moduli; comparison between the strain-dependent shear moduli of uncross-linked and permanently cross-linked collagen network. This material is available free of charge via the Internet at http://pubs.acs.org.

AUTHOR INFORMATION

Corresponding Author

*E-mail: nicholas@nus.edu.sg.

ACKNOWLEDGMENTS

We thank Jamie Siew for the technical help with rheological measurements. This work was supported by the National University of Singapore grants R279-000-214-133 and R279-000-214-731 and the Singapore-MIT Alliance (SMA). N.A.K. was supported by NUS Graduate School for Integrative Sciences and Engineering (NGS) and the Global Enterprise for Micro-Mechanics and Molecular Medicine (GEM[4]). L.H.W. was supported by an SMA scholarship.

REFERENCES

(1) Pelham, R. J.; Wang, Y.-l. Cell locomotion and focal adhesions are regulated by substrate flexibility. *Proc. Natl. Acad. Sci. U.S.A.* **1997**, *94*, 13661−13665.

(2) Friedl, P. Dynamic imaging of cellular interactions with extracellular matrix. *Histochem. Cell Biol.* **2004**, *122*, 183−190.

(3) Engler, A. J.; Sen, S.; Sweeney, H. L.; Discher, D. E. Matrix elasticity directs stem cell lineage specification. *Cell* **2006**, *126*, 677−689.

(4) Zaman, M. H.; Trapani, L. M.; Sieminski, A. L.; Siemeski, A.; Mackellar, D.; Gong, H.; Kamm, R. D.; Wells, A.; Lauffenburger, D. A.; Matsudaira, P. Migration of tumor cells in 3D matrices is governed by matrix stiffness along with cell-matrix adhesion and proteolysis. *Proc. Natl. Acad. Sci. U.S.A.* **2006**, *103*, 10889−10894.

(5) Solon, J.; Levental, I.; Sengupta, K.; Georges, P. C.; Janmey, P. A. Fibroblast adaptation and stiffness matching to soft elastic substrates. *Biophys. J.* **2007**, *93*, 4453−4461.

(6) Kasza, K. E.; Rowat, A. C.; Liu, J.; Angelini, T. E.; Brangwynne, C. P.; Koenderink, G. H.; Weitz, D. A. The cell as a material. *Curr. Opin. Cell Biol.* **2007**, *19*, 101−107.

(7) Gardel, M. L.; Shin, J. H.; MacKintosh, F. C.; Mahadevan, L.; Matsudaira, P.; Weitz, D. A. Elastic behavior of cross-linked and bundled actin networks. *Science* **2004**, *304*, 1301−1305.

(8) Lin, Y.-C.; Koenderink, G. H.; MacKintosh, F. C.; Weitz, D. A. Viscoelastic properties of microtubule networks. *Macromolecules* **2007**, *40*, 7714−7720.

(9) Storm, C.; Pastore, J. J.; MacKintosh, F. C.; Lubensky, T. C.; Janmey, P. A. Nonlinear elasticity in biological gels. *Nature* **2005**, *435*, 191−194.

(10) Gillette, B. M.; Jensen, J. A.; Tang, B.; Yang, G. J.; Bazargan-Lari, A.; Zhong, M.; Sia, S. K. In situ collagen assembly for integrating microfabricated three-dimensional cell-seeded matrices. *Nat. Mater.* **2008**, *7*, 636−640.

(11) Kaufman, L. J.; Brangwynne, C. P.; Kasza, K. E.; Filippidi, E.; Gordon, V. D.; Deisboeck, T. S.; Weitz, D. A. Glioma expansion in collagen I matrices: analyzing collagen concentration-dependent growth and motility patterns. *Biophys. J.* **2005**, *89*, 635−650.

(12) Vader, D.; Kabla, A.; Weitz, D.; Mahadevan, L. Strain-induced alignment in collagen gels. *PLoS ONE* **2009**, *4*, e5902.

(13) Arevalo, R. C.; Urbach, J. S.; Blair, D. L. Size-dependent rheology of type-I collagen networks. *Biophys. J.* **2010**, *99*, L65−L67.

(14) Stein, A. M.; Vader, D. A.; Weitz, D. A.; Sander, L. M. The micromechanics of three-dimensional collagen-I gels. *Complexity* **2010**, *16*, 22−28.

(15) Fung, Y.-C. *Biomechanics: Mechanical Properties of Living Tissues*; Springer-Verlag: New York, 1993.

(16) Silver, F. H. *Biological Materials: Structure, Mechanical Properties and Modeling of Soft Tissues*; New York University Press: New York, 1987.

(17) Yang, Y.-l.; Kaufman, L. J. Rheology and confocal reflectance microscopy as probes of mechanical properties and structure during collagen and collagen/hyaluronan self-assembly. *Biophys. J.* **2009**, *96*, 1566−1585.

(18) Franck, A. J. *Understanding Instrument Inertia Corrections in Oscillation*; TA Instruments: New Castle, DE, 2005.
(19) Piechocka, I. K.; van Oosten, A. S. G.; Breuls, R. G. M.; Koenderink, G. H. Rheology of heterotypic collagen networks. *Biomacromolecules* **2011**, *12*, 2797−2805.
(20) Schopferer, M.; Bar, H.; Hochstein, B.; Sharma, S.; Mucke, N.; Herrmann, H.; Willenbacher, N. Desmin and vimentin intermediate filament networks: their viscoelastic properties investigated by mechanical rheometry. *J. Mol. Biol.* **2009**, *388*, 133−143.
(21) Barocas, V. H.; Moon, A. G.; Tranquillo, R. T. The fibroblast-populated collagen microsphere assay of cell traction force--Part 2: Measurement of the cell traction parameter. *J. Biomech. Eng.* **1995**, *117*, 161−170.
(22) Raub, C. B.; Unruh, J.; Suresh, V.; Krasieva, T.; Lindmo, T.; Gratton, E.; Tromberg, B. J.; George, S. C. Image correlation spectroscopy of multiphoton images correlates with collagen mechanical properties. *Biophys. J.* **2008**, *94*, 2361−2373.
(23) Knapp, D. M.; Barocas, V. H.; Moon, A. G.; Yoo, K.; Petzold, L. R.; Tranquillo, R. T. Rheology of reconstituted type I collagen gel in confined compression. *J. Rheol.* **1997**, *41*, 971−993.
(24) Velegol, D.; Lanni, F. Cell traction forces on soft biomaterials. I. Microrheology of type I collagen gels. *Biophys. J.* **2001**, *81*, 1786−1792.
(25) Dorfmann, A.; Ogden, R. W. A constitutive model for the Mullins effect with permanent set in particle-reinforced rubber. *Int. J. Solids Struct.* **2004**, *41*, 1855−1878.
(26) Ewoldt, R. H.; Hosoi, A. E.; McKinley, G. H. New measures for characterizing nonlinear viscoelasticity in large amplitude oscillatory shear. *J. Rheol.* **2008**, *52*, 1427−1458.
(27) Gardel, M. L.; Nakamura, F.; Hartwig, J. H.; Crocker, J. C.; Stossel, T. P.; Weitz, D. A. Prestressed F-actin networks cross-linked by hinged filamins replicate mechanical properties of cells. *Proc. Natl. Acad. Sci. U.S.A.* **2006**, *103*, 1762−1767.
(28) Wilhelm, M. Fourier-Transform rheology. *Macromol. Mater. Eng.* **2002**, *287*, 83−105.
(29) Xu, D. H.; Craig, S. L. Strain hardening and strain softening of reversibly cross-linked supramolecular polymer networks. *Macromolecules* **2011**, *44*, 7478−7488.
(30) Orakdogen, N.; Erman, B.; Okay, O. Evidence of strain hardening in DNA gels. *Macromolecules* **2010**, *43*, 1530−1538.
(31) Ma, L.; Yamada, S.; Wirtz, D.; Coulombe, P. A. A 'hot-spot' mutation alters the mechanical properties of keratin filament networks. *Nat. Cell Biol.* **2001**, *3*, 503−506.
(32) Trepat, X.; Deng, L.; An, S. S.; Navajas, D.; Tschumperlin, D. J.; Gerthoffer, W. T.; Butler, J. P.; Fredberg, J. J. Universal physical responses to stretch in the living cell. *Nature* **2007**, *447*, 592−595.
(33) Rubinstein, M.; Panyukov, S. Elasticity of polymer networks. *Macromolecules* **2002**, *35*, 6670−6686.
(34) Onck, P. R.; Koeman, T.; van Dillen, T.; van der Giessen, E. Alternative explanation of stiffening in cross-linked semiflexible networks. *Phys. Rev. Lett.* **2005**, *95*, 178102.
(35) Huisman, E. M.; van Dillen, T.; Onck, P. R.; van der Giessen, E. Three-dimensional cross-linked f-actin networks: relation between network architecture and mechanical behavior. *Phys. Rev. Lett.* **2007**, *99*, 208103.
(36) Franck, C.; Hong, S.; Maskarinec, S. A.; Tirrell, D. A.; Ravichandran, G. Three-dimensional full-field measurements of large deformations in soft materials using confocal microscopy and digital volume correlation. *Exp. Mech.* **2007**, *47*, 427−438.
(37) Ewoldt, R. H.; Winter, P.; Maxey, J.; McKinley, G. H. Large amplitude oscillatory shear of pseudoplastic and elastoviscoplastic materials. *Rheol. Acta* **2010**, *49*, 191−212.
(38) Silver, F. H.; Ebrahimi, A.; Snowhill, P. B. Viscoelastic properties of self-assembled type I collagen fibers: Molecular basis of elastic and viscous behaviors. *Connect. Tissue Res.* **2002**, *43*, 569−580.
(39) Vader, D.; Muenster, S.; Jawerth, L.; Stein, A.; Weitz, D. Large amplitude oscillatory shear in collagen rheology shows early strain stiffening. *J. Biomech.* **2008**, *41*, S318.
(40) Schoenberg, M. Equilibrium muscle cross-bridge behavior. Theoretical considerations. *Biophys. J.* **1985**, *48*, 467−475.
(41) Wachsstock, D. H.; Schwarz, W. H.; Pollard, T. D. Cross-linker dynamics determine the mechanical properties of actin gels. *Biophys. J.* **1994**, *66*, 801−809.
(42) Kluge, J. A.; Thurber, A.; Leisk, G. G.; Kaplan, D. L.; Dorfmann, A. L. A model for the stretch-mediated enzymatic degradation of silk fibers. *J. Mech. Behav. Biomed. Mater.* **2010**, *3*, 538−547.
(43) Erk, K. A.; Henderson, K. J.; Shull, K. R. Strain stiffening in synthetic and biopolymer networks. *Biomacromolecules* **2010**, *11*, 1358−1363.
(44) van der Rijt, J. A. J.; van der Werf, K. O.; Dijkstra, P. J.; Bennink, M. L.; Feijen, J. Micromechanical testing of individual collagen fibrils. *Macromol. Biosci.* **2006**, *6*, 697−702.
(45) Puxkandl, R.; Zizak, I.; Paris, O.; Keckes, J.; Tesch, W.; Bernstorff, S.; Purslow, P.; Fratzl, P. Viscoelastic properties of collagen: synchrotron radiation investigations and structural model. *Philos. Trans. R. Soc., B* **2002**, *357*, 191−197.
(46) Ng, T. S. K.; McKinley, G. H.; Ewoldt, R. H. Large amplitude oscillatory shear flow of gluten dough: a model power-law gel. *J. Rheol.* **2011**, *55*, 627−654.
(47) Ewoldt, R. H.; Winegard, T. M.; Fudge, D. S. Non-linear viscoelasticity of hagfish slime. *Int. J. Non-Linear Mech.* **2011**, *46*, 627−636.